Regulation of an Enzyme by Phosphorylation at the Active Site

JAMES H. HURLEY,* ANTONY M. DEAN, JULIE L. SOHL, DANIEL E. KOSHLAND, JR., ROBERT M. STROUD

The isocitrate dehydrogenase of *Escherichia coli* is an example of a ubiquitous class of enzymes that are regulated by covalent modification. In the three-dimensional structure of the enzyme-substrate complex, isocitrate forms a hydrogen bond with Ser^{113}, the site of regulatory phosphorylation. The structures of Asp^{113} and Glu^{113} mutants, which mimic the inactivation of the enzyme by phosphorylation, show minimal conformational changes from wild type, as in the phosphorylated enzyme. Calculations based on observed structures suggest that the change in electrostatic potential when a negative charge is introduced either by phosphorylation or site-directed mutagenesis is sufficient to inactivate the enzyme. Thus, direct interaction at a ligand binding site is an alternative mechanism to induced conformational changes from an allosteric site in the regulation of protein activity by phosphorylation.

PROTEIN PHOSPHORYLATION IS OF CENTRAL IMPORTANCE IN metabolism, signal transduction, and many other cellular processes (*1*). Yet the three-dimensional structures of both the phosphorylated and dephosphorylated states are available for only two enzymes, glycogen phosphorylase (*2*) and isocitrate dehydrogenase (IDH) [threo-D$_s$-isocitrate:NAD(P)$^+$ oxidoreductase (decarboxylating); E.C. 1.1.1.42] (*3, 4*). Phosphorylation of glycogen phosphorylase enhances activity by means of long-range conformational changes (*2*). An understanding of the structural basis of a very different response in isocitrate dehydrogenase, complete inactivation by phosphorylation (*5*), has been hindered by the lack of knowledge of the active site. In order to locate the active site in relation to the phosphorylation site, we determined the structure of a complex of dephosphorylated IDH with magnesium isocitrate.

Inactivation by phosphorylation of Ser^{113} in IDH is mimicked when aspartate (*6*) or glutamate (*7*) is substituted at this site. In both cases, the binding of isocitrate is inhibited (*7, 8*). To clarify the mechanism of inactivation, we determined the three-dimensional structures of the S113D and S113E mutants and compared them with those of the phosphorylated and dephosphorylated enzymes.

Structure determination. To obtain a crystalline complex of IDH with substrate and to determine unambiguously the metal binding site, IDH crystals (*3*) were soaked in solutions containing isocitrate and either Mg^{2+} or Mn^{2+}. X-ray reflection data were collected to 2.5 Å resolution (Table 1). The metal ion was located at the largest peak (11 σ) in an $[F_o(\mathrm{Mn}) - F_o(\mathrm{Mg})]\alpha_{calc}$ Fourier difference map, with phases calculated from the refined structure of free IDH. $[F_o(\mathrm{Mn}) - F_o(\mathrm{free})]\alpha_{calc}$ and $[F_o(\mathrm{Mg}) - F_o(\mathrm{free})]\alpha_{calc}$ difference maps showed a large negative peak ($-16\ \sigma$) at the position of water-417 in the free enzyme, an indication that this water was displaced in the substrate-bound enzyme. Water-417 was removed and the Mg^{2+} ion was placed at the major peak in the $[F_o(\mathrm{Mn}) - F_o(\mathrm{Mg})]\alpha_{calc}$ Fourier difference map. Before refinement, an *R* factor of 0.239 was calculated with respect to amplitudes for the Mg isocitrate complex. This structure was then refined (*9*) to an *R* factor of 0.184. The 2R,3S-isocitrate, which is the biologically relevant isomer (*10*), was placed in an $[F_o(\mathrm{Mg}) - F_c]\alpha_{calc}$ difference map (Fig. 1) with amplitudes and phases calculated from the refined Mg complex structure, and the structure was refined to a final *R* factor of 0.176. The S113D and S113E mutants were crystallized as for wild type (*3*), and data were collected in the absence of ligands. The aspartate and glutamate side chains were located in $[F_o(\mathrm{mutant}) - F_o(\mathrm{WT})]\alpha_{calc}$ difference maps (Fig. 1) with phases calculated from wild type, and the structures were refined to final *R* factors of 0.163 at 2.8 Å and 0.179 at 2.4 Å, respectively. Crystals of the S113E mutant were soaked in the same solution of Mg^{2+} isocitrate that was used to obtain the wild-type enzyme-substrate complex. The S113E enzyme-substrate complex structure was built starting from structures for free S113E and the wild-type complex, adjusted with the aid of $[F_o(\mathrm{S113E\ complex}) - F_c(\mathrm{S113E\ free})]\alpha_{calc}$ (Fig. 1) and $[F_o(\mathrm{S113E\ complex}) - F_c(\mathrm{WT\ complex})]\alpha_{calc}$ difference maps, and refined to an *R* factor of 0.168 at 2.5 Å.

Structure of the enzyme-substrate complex. Isocitrate binds in a pocket between the two major domains of IDH, in which both subunits of the dimer participate (Fig. 2). Hydrogen bonds (2.6 Å $< d <$ 3.1 Å) are formed between isocitrate and Ser^{113}, Arg^{119}, Arg^{129}, Arg^{153}, Tyr^{160}, Lys$^{230'}$ [the prime sign (′) indicates the second subunit], and two bound water molecules. The Mg^{2+} is coordinated by isocitrate, Asp$^{283'}$, Asp^{307}, and two bound water molecules in a roughly octahedral manner. The coordination of Mg^{2+} to the α-carboxylate and the hydroxyl oxygen O7 of isocitrate positions the metal ion to play the key role in catalysis (*11*). Structural changes from the unliganded enzyme are local, the largest being movements of the side chains of Arg^{119} and Arg^{129} by as much

J. H. Hurley, J. L. Sohl, and R. M. Stroud, Department of Biochemistry and Biophysics and Graduate Group in Biophysics, University of California at San Francisco, San Francisco, CA 94143–0448. A. M. Dean and D. E. Koshland, Jr., Department of Molecular and Cell Biology, University of California at Berkeley, Berkeley, CA 94720.

*Present address: Institute of Molecular Biology, University of Oregon, Eugene, OR 97403.

as 2.1 Å in which the guanidino groups approach each other and the isocitrate molecule more closely.

Structures of phosphorylation site mutants. No atom of the active site residues 115, 119, 129, 153, 160, 230, 283, or 307 moves more than 0.8 Å between the S113D and S113E mutants and wild-type IDH (Fig. 3). The root-means-square shifts for active site residues excluding Ser^{113} are 0.25 Å and 0.21 Å, respectively. The movements of Tyr^{160} and Wat^{417} observed in phosphorylated IDH (*4*) do not occur in S113D and S113E; Tyr^{160} and Wat^{417} occupy positions in the S113D and S113E structures more similar to the dephosphorylated enzyme than the phosphorylated or substrate-bound forms. In contrast to results reported for the HPr protein (*12*), in which similar shifts in two-dimensional NMR spectra indicated similar structural changes on phosphorylation or replacement of serine by aspartate, structural changes on phosphorylation of IDH are not mimicked by the S113D replacement. These structural changes therefore cannot be the cause of inactivation. The hydroxyl oxygen of Tyr^{160} in phosphorylated IDH is 0.5 Å from the same atom in the substrate-bound structure, but 0.9 Å away from this atom in the S113D and free structures. The observation that the conformation of Tyr^{160} in the substrate-bound form is similar to that in the phosphorylated form is further evidence that small conformational changes seen on phosphorylation (*4*) are inessential for regulation.

The relative activities of uncharged and positively charged site-directed mutants at position 113 (*6–8*) can be explained by the observation that the phosphorylatable serine forms a hydrogen bond with isocitrate. Threonine can still form a hydrogen bond, but must rotate because of steric hindrance of Cγ by Val^{116}, and thus the hydroxyl is moved to a less favorable position. Alanine cannot form a hydrogen bond, but may accommodate a water molecule near the position occupied by Oγ of serine in wild-type IDH. Cysteine, tyrosine, and lysine are likely to be sterically unfavorable for isocitrate binding because of the size of these side chains. Models for S113C and S113K mutants, both of which have reduced but sizable activities, appear able to accommodate isocitrate binding solely by rotations of the side chain at residue 113. However, a tyrosine side chain at residue 113 cannot be accommodated without both main chain and side chain adjustments. Steric disruption of binding by tyrosine and lysine side chains, comparable in size to a serine phosphate, accounts for an additional reduction in affinity. The relatively small changes in the activity of the uncharged and positively charged mutant enzymes can be accounted for by the loss of a hydrogen bond and unfavorable steric interactions. This suggests that the large loss in activity that occurs on phosphorylation must have a large electrostatic component.

Despite the very low affinity of the S113E mutant for isocitrate at physiological pH and ionic strength (*7*), isocitrate binds to this mutant at the high ionic strength (6.9 M) and high isocitrate concentration (100 mM) used to obtain a crystalline complex. Isocitrate is sterically accommodated in the active site by movements of up to 1.6 Å by both the Glu^{113} side chain and the γ-carboxylate of

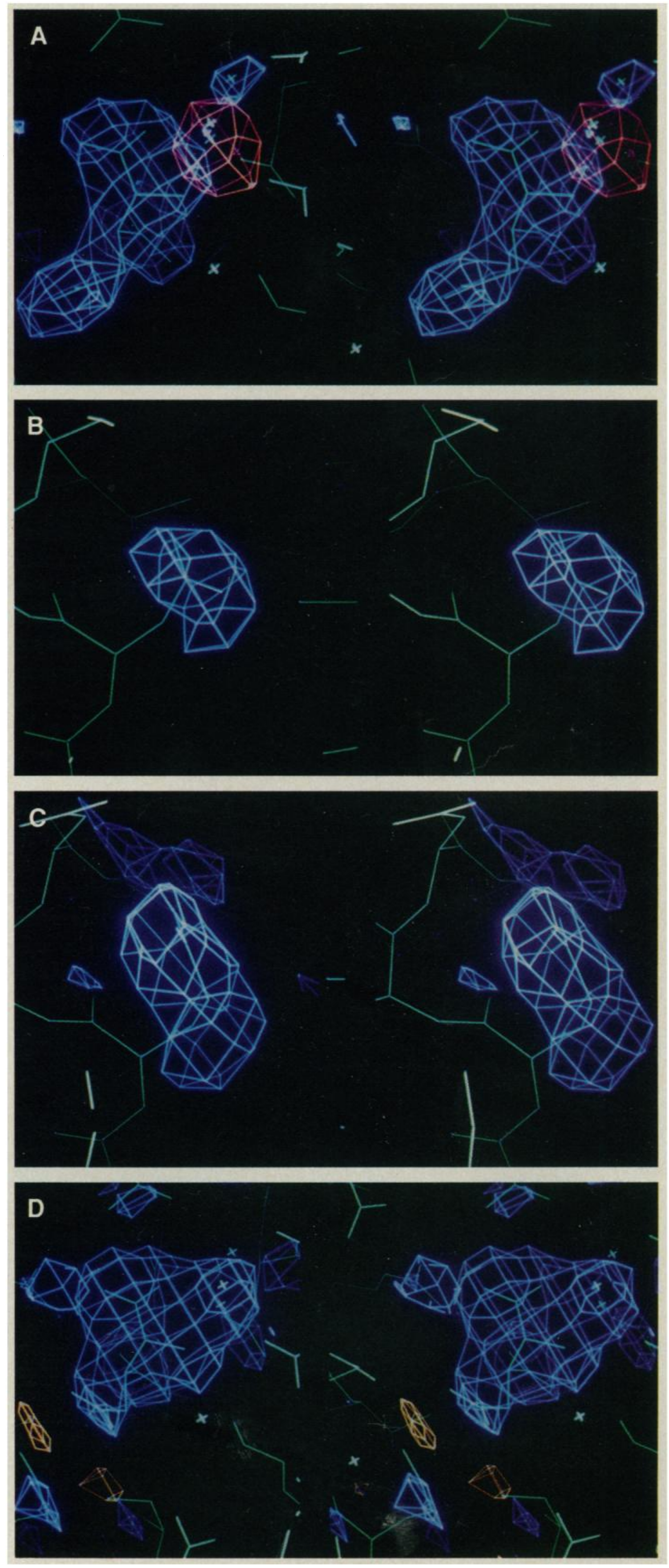

Fig. 1. (**A**) Isocitrate in electron density (blue) from a $[F_o(Mg) - F_c]\alpha_{calc}$ difference map at 2.5 Å resolution with amplitudes and phases calculated from a structure refined after including Mg^{2+} but not isocitrate. $[F_o(Mn) - F_o(Mg)]\alpha_{calc}$ difference density is shown in red. Maps are displayed with FRODO (*18*), contoured at 5 σ and superimposed on the refined structure of the Mg^{2+} isocitrate complex. Crosses indicate the metal ion and adjacent water molecules. X-ray intensity data were collected for IDH crystals soaked for at least 3 hours in solutions of 100 mM 2*R*, 3*S*-isocitric acid (monopotassium salt, Sigma), either 10 mM $MgSO_4$ or 10 mM $MnCl_2$, 100 mM NaCl, 35 mM Na_2HPO_4, 2 mM DTT, and 0.02 percent NaN_3 in 50 percent saturated $(NH_4)_2SO_4$, at pH adjusted to 6.0 with concentrated NH_4OH. Local scaling (*19*) was used for all map calculations. (**B**) At 2.8 Å resolution $[F_o(S113D) - F_o(\text{wild type})]\alpha_{calc}$ difference map, contoured at 3.5 σ and superimposed on the refined structure of the S113D mutant. (**C**) At 2.5 Å resolution, $[F_o(S113E\ \text{free}) - F_o(\text{wild type})]\alpha_{calc}$ difference map contoured at 4 σ and superimposed on the refined structure of the S113E mutant. (**D**) At 2.5 Å resolution $[F_o(S113E\ \text{complex}) - F_c(S113E\ \text{free})]\alpha_{calc}$ difference map contoured at ±3 σ and superimposed on the refined structure of the S113E complex. Blue and red indicate positive and negative difference density, respectively.

isocitrate (Fig. 3). The γ-carboxylate becomes more mobile in the S113E complex, with *B* factors increasing from 32 to 38 in the wild-type complex to 45 to 50. The O4 of isocitrate is within 3.0 Å of Glu^{113} in the complex, but the geometry is not favorable for formation of a hydrogen bond by a protonated form of either isocitrate or Glu^{113}. The unfavorable geometry for isocitrate binding in the active site of S113E may lead to a reduced affinity for the substrate even under conditions in which the role of electrostatic interactions is expected to be minimal.

Electrostatic effect of phosphorylation on isocitrate binding. To determine whether a direct electrostatic interaction with the substrate could account for the effect of introducing a negative charge at position 113, we used numerical solution of the Poisson-Boltzmann equation as developed by Honig and co-workers (*13*) to calculate the change in the electrostatic free energy of binding of the magnesium (Mg^{2+}) isocitrate complex produced by either phosphorylation or replacement of serine by aspartate or glutamate (*14*). Magnesium and isocitrate bind to $NADP^+$-dependent IDH as a complex (*15*). Calculations were based on the structure of the S113E enzyme-substrate complex. Model structures of phosphorylated IDH and S113D complexed with isocitrate were also built on the basis of the structures of substrate-bound wild-type IDH, and of phosphorylated IDH and S113D in the absence of substrate. When the Mg^{2+} isocitrate structure is superimposed on the phosphorylated IDH and S113D structures to construct a model complex, distances from the γ-carboxylate of isocitrate to the nearest phosphate or carboxylate oxygen of residue 113 are less than 2.4 Å. When rotations in main chain and side chain torsion angles for residue 113 are allowed, in a manner similar to that seen in the crystal structure of the S113E complex, a complex with either the phosphorylated or S113D enzymes can be accommodated without unreasonably close contacts.

The calculated change in electrostatic free energy of binding of

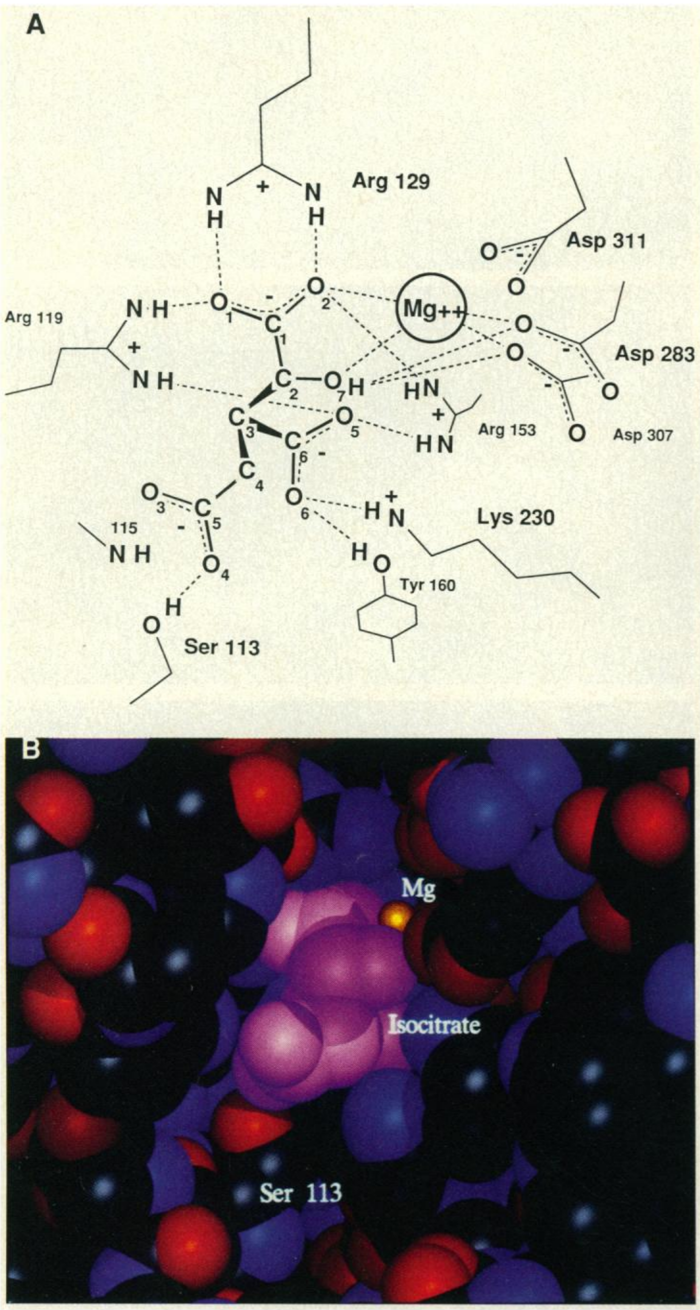

Fig. 2. (**A**) Mg^{2+} isocitrate bound in the active site of IDH. Hydrogens are shown for illustrative purposes where hydrogen bonds between enzyme and substrate are thought to occur. Dashed lines indicate likely hydrogen bonds or salt bridges. Residues of the second subunit are indicated by a prime. Water molecules are not shown. (**B**) Space-filling model of the active site of IDH, showing the same view as (A). For the enzyme, carbon is colored black, oxygen red, and nitrogen blue. Isocitrate is colored pink and Mg^{2+} yellow.

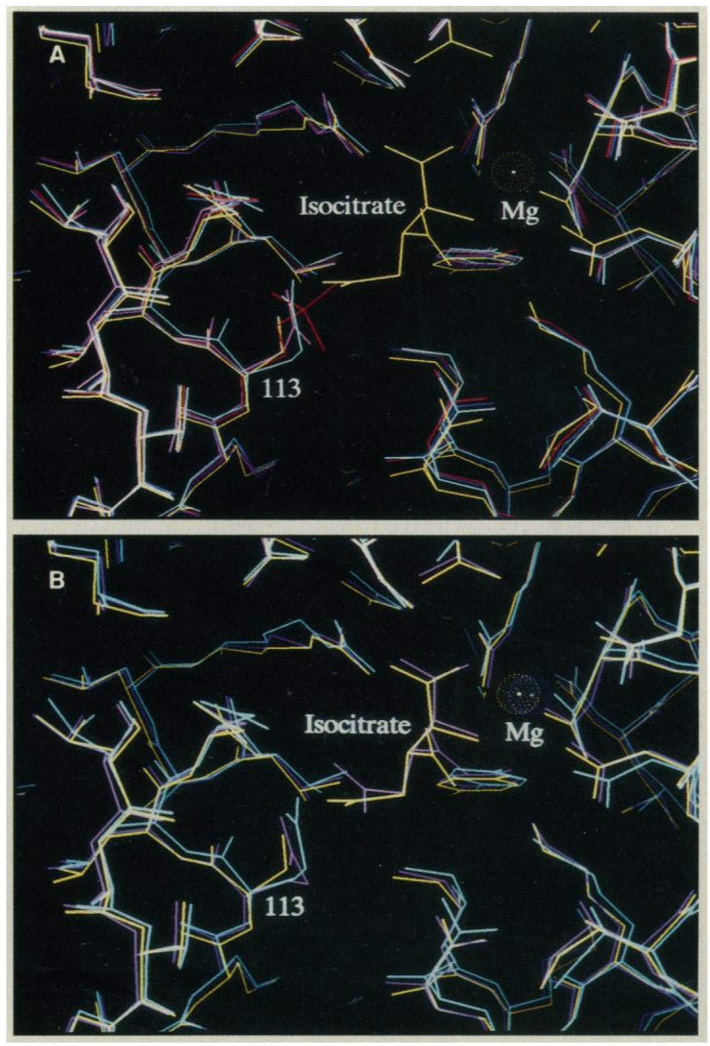

Fig. 3. (**A**) Structures of substrate-bound IDH (yellow), and unliganded IDH (blue), phosphorylated IDH (red), S113D (magenta), and S113E (cyan). (**B**) Structures of substrate-bound S113E (purple) and wild-type IDH (yellow), and unliganded S113E (cyan), showing the movements of the Glu^{113} side chain and the γ-carboxylate of isocitrate.

Table 1. Crystallographic statistics. All x-ray intensity data were collected with a Nicolet area detector and reduced with the XENGEN package (*16*). Structures were refined with XPLOR minimization (*9*) and manual rebuilding into $(2F_o - F_c)_{\alpha calc}$ electron density maps. Energy parameters were obtained from the CHARMM library (*17*) normally used with XPLOR, except that van der Waals parameters were added for Mg^{2+} and improper angles for the two chiral centers of isocitrate were calculated from the small molecule structure (*10*). $R_{cryst} = \Sigma|F_o - F_c|/\Sigma F_o$, where reflections with $F/\sigma(F) > 1.0$ and $d < 5.0$ Å were used in refinement and R factor calculation. The percentage of reflections with $F/\sigma(F) > 1.0$ is shown for all measured reflections. $R_{merge} = \Sigma|I_i - \langle I \rangle|/\Sigma\langle I \rangle$, summed over all observations from all crystals. Space group: $P4_32_12$. Cell dimensions: $a = b$ 105.1 Å; c = 150.3 Å.

	Unique reflections		Total obser-vations	Reflections $F/\sigma(F) > 1.0$ (%)	R merge	R_{cryst}	Δbond rms (Å)	Δangle rms (deg)	Resolu-tion (Å)
	Possible (*N*)	Collected (*N*)							
Mg complex	30274	29506	111257	78.6	0.144*	0.176	0.019	3.4°	2.5
Mn complex	30274	13048	31102	88.9	0.094				2.5
S113D free	21721	20711	89070	79.5	0.204*	0.163	0.016	3.3°	2.8
SII3E free	34306	27716	67344	82.6	0.099	0.179	0.016	3.1°	2.4
S113E complex	30274	26412	62251	83.8	0.093	0.168	0.016	3.1°	2.5

*Data were collected for only one crystal each for the Mn^{2+} complex and both S113E structures; three crystals each were used for collection of the other two data sets. All crystals used for data collection were at least 0.7 mm along the largest dimension, except for S113D crystals, which grew to no larger than 0.3 mm along the largest dimension.

Mg^{2+} isocitrate to S113E is $\Delta(\Delta G_{bind}) = +21$ kcal/mol (Table 2). Calculations were repeated for alternative model-built structures to determine the dependence of $\Delta(\Delta G_{bind})$ on structural changes. Models A, B, and C are based on maximal shifts of residue 113 or isocitrate which move negative charges as far apart as possible, rotating only the γ-carboxylate of isocitrate and the main chain and side chain at residue 113. In alternative models for phosphorylated IDH and S113D, $\Delta(\Delta G_{bind})$ is +5 to +13 kcal/mol. These calculations, although dependent on the use of the linearized Poisson-Boltzmann equation and the assumption that the polarizability of the protein interior is homogeneous and isotropic, suggest that the change in electrostatic potential could account for the large observed decrease in affinity for isocitrate.

Protonation of Asp^{113}, Glu^{113}, or phospho-Ser^{113} could substantially affect conclusions based on calculations of $\Delta(\Delta G_{bind})$ for the ionized forms of these side chains. Given the concentration of positive charge near residue 113 (Arg^{119}, Arg^{129}, Arg^{153}, and $Lys^{230'}$), it is unlikely that Asp^{113}, Glu^{113}, or phospho-Ser^{113} are predominantly uncharged at neutral pH, although phospho-Ser^{113} might be predominantly singly ionized. If one negative charge is still present on phospho-Ser^{113}, $\Delta(\Delta G_{bind})$ for isocitrate binding to the singly ionized species is one-half the value calculated for the doubly ionized serine phosphate in the linear Poisson-Boltzmann equation, if no assumption is made as to which phosphate oxygen is protonated. The tribasic metal-isocitrate complex is the principal substrate of $NADP^+$-dependent IDH (*15*). Protonated forms of isocitrate are believed to be kinetically unimportant under normal circumstances (*15*), but the metal-isocitrate complex has a pK_a of 5.7 (*15*); thus it cannot be ruled out that a protonated form is the principal substrate of S113D, S113E, and phosphorylated IDH. The low level of activity remaining for the S113D and S113E enzymes (*7*) may be due to a small concentration of either singly protonated metal-isocitrate complex or protonated Asp^{113} or Glu^{113} (*7*). This might account in part for the apparent discrepancy between the observed and calculated values for the electrostatic contribution to $\Delta(\Delta G_{bind})$.

In contrast to regulation of glycogen phosphorylase, in which phosphorylation far from the active site induces long-range conformational changes. IDH demonstrates that phosphorylation can act directly at a substrate binding site without inducing large structural changes. In IDH, the phosphorylatable serine is also an active site residue, demonstrating that it is possible for a protein kinase to act at the active site of an enzyme. Electrostatic potential calculations based on the structure of the enzyme-substrate complex and comparison to results of site-directed mutagenesis lead to the conclusion that the loss of a hydrogen bond with isocitrate and a combination of electrostatic and steric interactions between the serine phosphate and isocitrate are responsible for inhibition of the enzyme. Numerous examples of proteins for which phosphorylation alters affinity for a ligand have been reported. Thus, regulatory covalent modification may act by two alternative mechanisms, modification at an allosteric site or direct interaction of a covalently modified amino acid with a ligand, whether a small molecule or a macromolecule. The extent of usage of these alternatives remains to be determined.

Table 2. Electrostatic potential change ΔΦ at each fully charged atom in the Mg^{2+} isocitrate complex, and the change in electrostatic free energy of binding for Mg^{2+} isocitrate $\Delta(\Delta G_{bind})$, between each model and the wild-type dephosphorylated enzyme. $\Delta(\Delta G_{bind}) = \Sigma q_i \Delta\Phi_i$, summed over all full charges in the Mg^{2+} isocitrate complex. Atoms O1 and O2 belong to the α-carboxylate, O3 and O4 to the γ-carboxylate, and O5 and O6 to the β-carboxylate of isocitrate. "Crystal" refers to the calculation based on the crystallographic structure of the Mg^{2+} isocitrate complex with the S113E mutant. Model A is derived from the superposed structures of S113D and the wild-type Mg^{2+} isocitrate complex by rotating the γ-carboxylate as far as possible from residue 113, into an eclipsed conformation. In model B, the Asp^{113} side chain is moved as far as reasonably possible from isocitrate by a combination of main-chain and side-chain rotations. Models C and D are based on the phosphorylated IDH structure. In model C, phospho-Ser^{113} is moved as far as reasonably possible from isocitrate by a combination of main chain and side chain rotations. In model D, phospho-Ser^{113} is moved by approximately one-half the distance in model C, sufficient to remove steric overlap between isocitrate and the phospho-Ser^{113} side chain.

Atom	ΔΦ [kcal/(mol·e)]				
	Crystal	A	B	C	D
O1	−2.2	−3.0	−1.0	−1.3	−2.1
O2	−1.9	−2.6	−1.1	−1.2	−2.0
O3	−7.6	−3.1	−2.0	−2.7	−6.8
O4	−25.4	−2.1	−5.2	−5.2	−13.0
O5	−3.9	−5.7	−2.4	−2.0	−3.7
O6	−3.9	−5.9	−3.3	−2.4	−5.1
Mg	−1.2	−1.8	−0.8	−1.0	−1.6
	$\Delta(\Delta G_{bind})$ (kcal/mol)				
	21.0*	7.5	5.8	5.4	13.1

*$\Delta(\Delta G_{bind}) = 21 \pm 1$ kcal/mol is obtained by averaging the calculated $\Sigma q_i \Delta\Phi_i = 22$ kcal/mol for $\Delta\Phi_i$ at the Glu^{113} side chain due to charges on Mg^{2+} isocitrate and $\Sigma q_i \Delta\Phi_i = 20$ kcal/mole for $\Delta\Phi_i$ at Mg^{2+} isocitrate due to charges on Glu^{113}. As these two quantities are formally equal, the discrepancy is a measure of error in the finite-difference solution to the Poisson-Boltzmann equation.

REFERENCES AND NOTES

1. E. Krebs, in *The Enzymes*, P. D. Boyer and E. G. Krebs, Eds. (Academic Press, New York, ed. 3, 1986), vol. 17, pp. 3–18; A. M. Edelman, D. K. Blumenthal, E. G. Krebs, *Annu. Rev. Biochem.* **56**, 567 (1987).
2. S. R. Sprang *et al.*, *Nature* **336**, 215 (1988); E. J. Goldsmith, S. R. Sprang, R.

Hamlin, N.-H. Xuong, R. J. Fletterick, *Science* **245**, 528 (1989); D. Barford and L. N. Johnson, *Nature* **340**, 609 (1989).
3. J. H. Hurley *et al.*, *Proc. Natl. Acad. Sci. U.S.A.* **86**, 8635 (1989).
4. J. H. Hurley, A. M. Dean, P. E. Thorsness, D. E. Koshland, Jr., R. M. Stroud, *J. Biol. Chem.* **265**, 3599 (1990).
5. D. C. LaPorte and D. E. Koshland, Jr., *Nature* **305**, 286 (1983).
6. P. E. Thorsness and D. E. Koshland, Jr., *J. Biol. Chem.* **262**, 10422 (1987).
7. A. M. Dean and D. E. Koshland, Jr., *Science* **249**, 1044 (1990).
8. A. M. Dean, M. H. I. Lee, D. E. Koshland, Jr., *J. Biol. Chem.* **264**, 20482 (1989).
9. A. T. Brünger, K. Kuriyan, M. Karplus, *Science* **235**, 458 (1987).
10. D. van der Helm *et al.*, *Acta Crystallogr. Sect. B.* **24**, 578 (1968).
11. J. H. Hurley, A. M. Dean, D. E. Koshland, Jr., R. M. Stroud, in preparation.
12. M. Wittekind, J. Reizer, J. Deutscher, M. H. Saier, R. E. Klevit, *Biochemistry* **28**, 9908 (1989). HPr is the histidine-containing phosphocarrier protein of the PTS.
13. I. Klapper, R. Hagstrom, R. Fine, K. Sharp, B. Honig, *Proteins* **1**, 47 (1986); M. K. Gilson, K. A. Sharp, B. H. Honig, *J. Comp. Chem.* **9**, 327 (1988).
14. To test the accuracy of the calculations and their sensitivity to variable parameters, a series of trial calculations were made. In that our results were strongly dependent on the value of dielectric constant for the protein interior, we chose the value 4, which is at the high end of the range 2 to 4 normally considered appropriate (*13*). A dielectric constant of 80 was used for the solvent region. Treatment of solvent screening proved essential to obtain reasonable results; the increase in binding energy for model D calculated from Coulomb's law with a dielectric constant $\epsilon = 4$ was 48.6 kcal/mol, compared to 13.1 kcal/mol calculated with a solvent dielectric constant of 80 and nonzero I. The linearized Poisson-Boltzmann equation was used to calculate the potential due to the charges on Glu^{113}, Asp^{113}, or phospho-Ser^{113} alone. The ionic strength I of the buffer normally used for IDH activity assays and used in the calculation was 0.115 M; changing I to 0.145 M had a negligible effect on the calculated result. No ion exclusion layer was used for the calculations reported here, but the use of such a layer was found to have a minimal effect on the solution to the linear equation in trial calculations. Potentials were calculated by a three-step focusing procedure: the first calculation used a 6.25 Å grid spacing with Debye-Huckel boundary conditions, followed by calculations on grids with 1.25 and 0.625 Å spacings. Repeating the calculation on a 0.30 Å grid produced no further change in the result. The calculated $\Delta(\Delta G_{bind})$ was identical at 0.625 and 0.30 Å, and roughly 10 percent larger at 1.25 Å. All calculations were performed on a cubic grid with 65 units per side and iterations continued to convergence. $\Delta(\Delta G_{bind})$ calculated from multiple cycles of translational averaging varied from the mean by less than 2 percent.
15. See J. J. Marr and M. M. Weber [*Arch. Biochem. Biophys.* **158**, 782 (1973)] for data on nicotinamide adenine dinucleotide phosphate ($NADP^+$)–dependent IDH from *Salmonella typhimurium*; see R. S. Ehrlich and R. F. Colman [*Biochemistry* **26**, 3461 (1987); *ibid.*, **28**, 2058 (1989)] for data on NADP-dependent IDH from pig heart, pK_a value for Cd^{2+} isocitrate.
16. A. J. Howard *et al.*, *J. Appl. Cryst.* **20**, 383 (1987).
17. B. R. Brooks *et al.*, *J. Comp. Chem.* **4**, 187 (1983).
18. T. A. Jones, *Methods Enzymol.* **115**, 157 (1985).
19. J. H. Hurley and R. M. Stroud, unpublished program.
20. We thank K. Sharp, A. Nicholls, and B. Honig for use of their program DELPHI; P. Thorsness for assistance in preparing S113D IDH; B. Shoichet for assistance with obtaining small molecule structures; and J. Day for helpful discussions of protein-metal interactions. Figures 2B and 3 were created by J. Newdoll, using software written by C. Huang, E. Pettersen, and G. Couch at the UCSF Computer Graphics Lab. Supported by NIH grant GM 24485 (R.M.S.); NSF grant 04200 (D.E.K.); a grant from the Lucille P. Markey Charitable Trust (D.E.K.); a U.C. Regent's fellowship (J.H.H.); and an NSF fellowship (J.L.S.). Crystallographic refinement was carried out at the Pittsburgh Supercomputer Center under grant DMB890040P. Coordinates for the Mg^{2+} isocitrate complex and the S113D and S113E mutants have been deposited with the Protein Data Bank at Brookhaven.

10 April 1990; accepted 19 July 1990

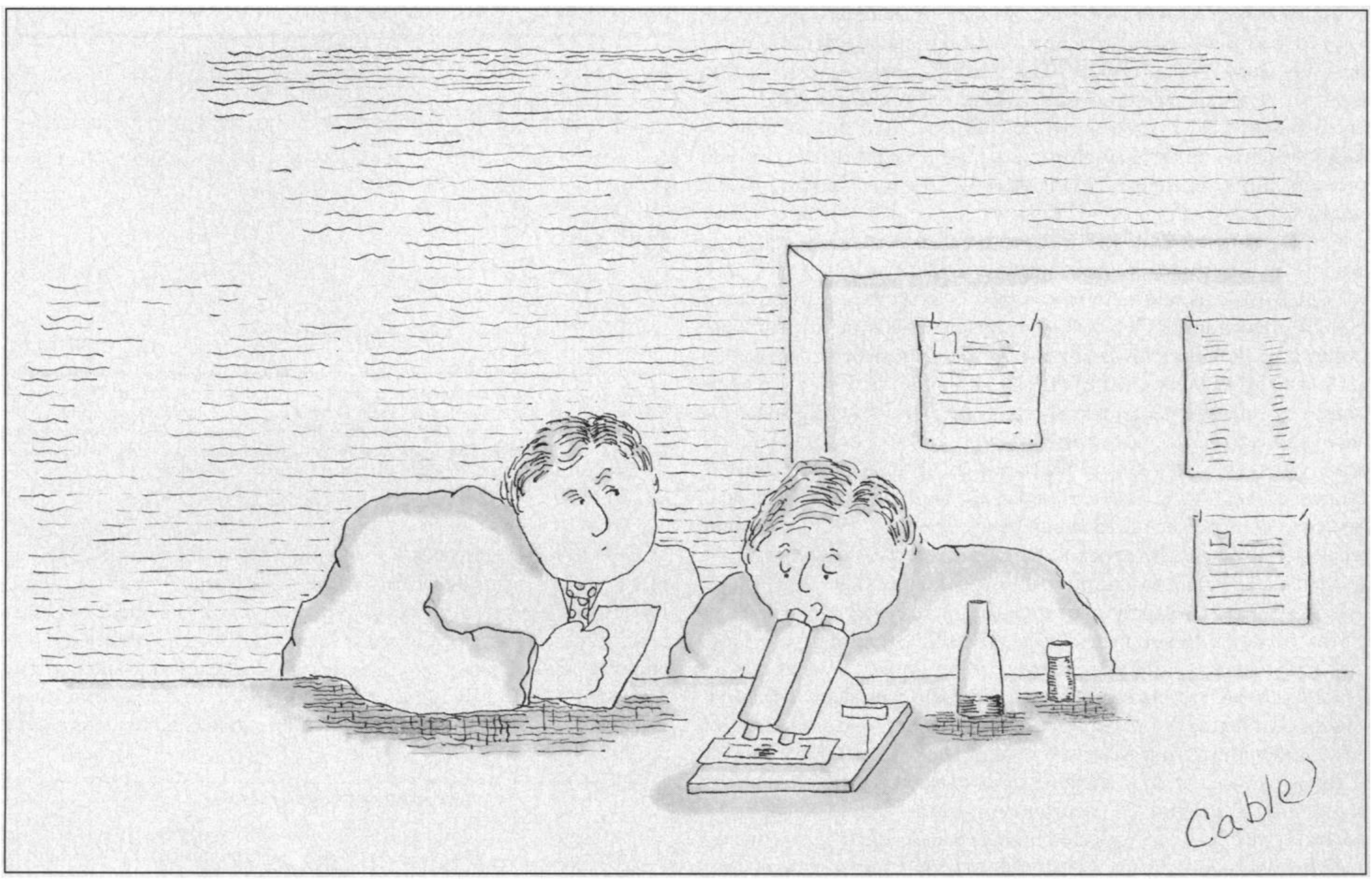

"The oil-eating bacteria prefer premium to regular and caviar to premium."